Structural, electrical, and vibrational properties of Ti-H and Ni-H complexes in Si

D. J. Backlund and S. K. Estreicher*
Physics Department, Texas Tech University, Lubbock, Texas 79409-1051, USA
(Received 28 May 2010; revised manuscript received 24 September 2010; published 19 October 2010)

Hydrogen passivates many electrically active impurities in Si. While most passivation reactions are understood experimentally and theoretically, the interactions between H and transition-metal (TM) impurities of the 3*d* series are poorly understood. H does trap at various TMs but new electrically active levels in the gap appear following hydrogenation. No specific complex has been assigned to any of these new lines and even the number of hydrogen atoms involved is only assumed. Electrical studies of Ti-H and Ni-H interactions have sometimes produced conflicting results. We report here the results of systematic first-principles studies of Ti-H and Ni-H interactions in Si. The stable structures, binding energies, electrical properties, and vibrational spectra are predicted. Several of the observed complexes are identified. We find one electrically inactive Ti-H complex, $\{Ti_iH_4\}$, but no inactive Ni-H complex. We show that, if enough H is available, substitutional Ti and Ni are expelled to interstitial sites, leaving a partially H-saturated vacancy.

DOI: 10.1103/PhysRevB.82.155208 PACS number(s): 61.72.−y, 71.55.−i

I. INTRODUCTION

Hydrogen is a fast-diffusing interstitial impurity in Si which interacts covalently with a wide range of defects.[1–3] Because of the strength of many chemical bonds involving H, the bonding-antibonding separation often exceeds the Si band gap. As a result, the electrically active gap levels of numerous defect centers shift upon hydrogenation, sometimes within the gap but often into the valence or conduction bands, thus passivating the defect.

Hydrogen is commonly used to increase minority-carrier lifetimes in photovoltaic- (PV-) grade Si, especially in *p*-type material.[4,5] In particular, the heat treatment which follows the plasma-enhanced chemical-vapor deposition of an SiN_x layer (antireflection coating) injects hydrogen into the bulk of the material.[6,7] Even though it is not known which defects are passivated, the lifetime of minority carrier often increases substantially.

The transition metals (TMs) from the 3*d* series are among the most feared impurities in PV- and integrated circuit-grade Si's. These common contaminants, often present in the source material, can be introduced into the material during various processing steps (metal contacts, surface layers, impurities in furnaces, etc.). These TMs are often associated with strong recombination centers.[8–11] The lightest elements in the series (Ti and V) are very strong traps for minority carriers in *p*-Si (Refs. 26 and 27) and are also very slow interstitial diffusers, which makes them nearly impossible to getter. The heaviest elements in the series (Ni and Cu) are almost harmless when isolated but are among the fastest interstitial diffusers known.[12,13] They precipitate and these larger defects are electrically active.[14–18]

Deep-level transient spectroscopy (DLTS) has been used to study the interactions between hydrogen and a range of TM impurities.[19,20] In general, if H traps at a TM impurity, the gap levels of the TM shift within the gap but are not removed. A wide range of new deep levels associated with $\{TM,H_n\}$ complexes appear following hydrogenation. The structure and the number of H involved are known in only rare case.[21,22] Comparisons of the intensities of the DLTS peaks combined with annealing studies suggest that electrically inactive complexes exist in some cases. In this paper, we focus on the interactions between hydrogen and Ti or Ni.

Isolated interstitial titanium (Ti_i) is stable at the tetrahedral interstitial (*T*) site. It has double-donor, donor, and acceptor levels at level at $E_v+0.25$, $E_c-0.27=E_v+0.89$, and $E_c-0.09$ eV, respectively.[23,24] We calculate[13] these levels to be at $E_v+0.15$, $E_v+0.76$, and $E_c+0.07$ eV, respectively. The measured[25] activation energy for diffusion in intrinsic Si is 1.79 eV. Our calculations give 1.79 eV, 1.66 eV, 1.75 eV, and 1.66 eV for Ti_i in the ++, +, 0, and − charge state, respectively. In *p*-Si, this slow diffusing interstitial impurity is in the ++ charge state and a major killer of minority carriers.[26,27] The consequences of hydrogenating Ti-contaminated Si samples has been studied by two groups.

Singh *et al.*[28] implanted protons into moderately doped *p*-Si and *n*-Si, etched away the damaged surface layer, and annealed the sample at 300 °C before performing DLTS measurements. They report that no passivation of Ti occurs. However, Ti_i should be in the + or ++ charge state in their samples and H diffuses as H^+ as well. The long-ranged Coulomb repulsion reduces the probability of any H-Ti reaction. Further, as discussed below, a 300 °C anneal breaks up any Ti-H complex.

Jost *et al.*[29] introduced H into moderately doped *p*- and *n*-type Si by wet chemical etching as well as exposure to a remote hydrogen plasma, annealed the samples at 470 K, and performed DLTS experiments. In *n*-type samples, the DLTS spectrum shows four peaks. Two of them are associated with the acceptor and donor levels of isolated Ti_i. The other two peaks, $E_c-0.31$ and $E_c-0.57$ eV, are associated with near-surface defects. They anneal out after three hours at 570 K, but not in the 300–450 K range. Depth profiling provides evidence that the concentration of the $E_c-0.57$ eV level is greatest near the surface and decreases toward the bulk. The depth profile of the $E_c-0.31$ eV level could not be determined due to its strong overlap with the Ti_i donor level but a DLTS measurement deeper in the bulk confirms that this level lies in the surface region. When the *n*-type samples are treated in a hydrogen plasma, the DLTS spectrum is similar to that obtained after wet chemical etching, except that the

$E_c-0.31$ and $E_c-0.57$ eV peaks are more pronounced. These two peaks have been assigned to unspecified {Ti,H} complexes.

In *p*-type samples, three peaks in the DLTS spectrum correspond to the acceptor, donor, and double-donor levels of Ti_i. The concentration of the double donor is not affected by wet chemical etching, as H^+ passivates the shallow B^- acceptors instead. A zero-bias 400 K anneal breaks up the {B,H} pairs and then the concentration of the Ti double donor level drops near the surface. This decrease does not occur under reverse bias: the double-donor level is only passivated near the surface when minority carriers are available.

Finally, the authors[29] point out that, before the 570 K anneal, the sum of the DLTS amplitudes of the Ti and {Ti,H} lines is less than the prehydrogenation Ti concentration. The concentrations of the Ti_i acceptor and donor levels fully recover only following a 3 h, 570 K anneal. The authors propose that there is at least one electrically inactive Ti-H complex with a concentration greater than the concentration of the electrically active {Ti,H} levels.

The only published theoretical study[30] involving Ti and H in Si involved approximate *ab initio* and *ab initio* Hartree-Fock calculations in H-saturated clusters containing 10 or 35 Si atoms. The authors predicted that H binds to interstitial Ti with a binding energy of 2.3 eV but the electrical activity of the pair was not calculated.

Isolated interstitial nickel (Ni_i) is also stable at the *T* site. No gap level associated with it has been reported in the literature. We predicted[13] that the donor level is just below the top of the valence band and the acceptor level just above the bottom of the conduction band. Thus, isolated Ni_i should be in the 0 charge state for all positions of the Fermi level. The activation energy for diffusion was calculated to be 0.21 eV. The experimental values[31] for this migration barrier differ by more than a factor of 30, illustrating how difficult it is to measure the activation energy of an electrically neutral interstitial which diffuses very fast, even at low temperatures.

The interactions between Ni and H have been studied by DLTS (Ref. 32) in Ni-contaminated *p*- and *n*-type Si. The hydrogenation was done by wet chemical etching. A total of 14 DLTS peaks were observed, three of which match the double acceptor ($E_c-0.08$ eV), acceptor ($E_c-0.39$ eV), and donor ($E_v+0.15$ eV) levels of isolated substitutional Ni (Ni_s).[33–35] In addition to these DLTS peaks, the authors report six hole traps ($E_v+0.08$, 0.20, 0.32, 0.37, 0.47, 0.56 eV) and five electron traps ($E_c-0.15$, 0.16, 0.25, 0.35, 0.52 eV). These eleven new levels are attributed to unspecified Ni-H complexes because their appearance coincides with a reduction in the intensity of the isolated Ni_s DLTS peaks upon hydrogenation. In *n*-type Si, a one-hour anneal at 470 K reduces the amplitude of the electron traps and a 2 h anneal at 570 K recovers the original concentration of the Ni_s acceptor levels. In *p*-type samples, all the H-related hole traps also anneal out at 570 K but the Ni_s donor level does not fully recover.

The only published theoretical study[36] of Ni and H in Si involved density-functional calculations in H-saturated clusters containing 34–70 Si atoms. The authors predicted that the $\{Ni_sH_2\}$ complex has the two H's at the antibonding site of two Si nearest neighbors (NNs) to Ni_s. However, further calculations in periodic supercells have shown[37] that the antibonding configuration for H trapped at Ni_s is not the lowest energy structure. Instead, H attaches directly to the transition metal, as had been predicted for Cu_s.[38,39]

In this work, we present the results of first-principles calculations of the interactions of one or more H interstitials with Ti and Ni in Si.[40] The lowest energy configurations and their binding energies are predicted. The approximate position of the donor and acceptor levels of the stable complexes is calculated and several of the observed DLTS levels are assigned to specific complexes. We also predict the vibrational spectra of the most stable Ti-H and Ni-H complexes in order to facilitate future optical experimental identification. We also predict that, given a sufficiently high concentration of H, substitutional Ti and Ni are expelled to interstitial sites leaving a partially H-saturated vacancy. The level of theory is discussed in Sec. II. Sections III and IV contain the results for Ti-H and Ni-H interactions, respectively. The key points are discussed in Sec. V.

II. METHODOLOGY

A. Electronic structure

Our first-principles electronic structure and *ab initio* molecular-dynamics simulations,[41] based on the SIESTA method,[42,43] have been used in earlier studies of 3*d* TM impurities in Si.[13,44,45] The host crystal is represented by periodic supercells containing 216 host atoms. The lattice constant of the perfect cell is optimized in each charge state. The defect geometries are obtained with a conjugate gradient algorithm. A $3\times3\times3$ Monkhorst-Pack[46] mesh is used to sample the Brillouin zone.

The electronic core regions are removed from the calculations using *ab initio* norm-conserving pseudopotentials with the Troullier-Martins parameterization[47] in the Kleinman-Bylander form.[48] The SIESTA pseudopotentials have been optimized using the experimental bulk properties of the perfect solids and/or first-principles calculations[49] as well as vibrational properties of free molecules or known defects, when such experimental data are available. Such testing leads to some fine tuning of the pseudopotential parameters relative to the purely atomic ones: small changes in the core radii and/or use of semicore states. Once optimized, we take these pseudopotentials to be transferable to the defect problems at hand.

The valence regions are treated with first-principles spin-density-functional theory within the generalized gradient approximation for the exchange-correlation potential.[50] The charge density is projected on a real-space grid with an equivalent cutoff of 350 Ryd to calculate the exchange-correlation and Hartree potentials. The basis sets for the valence states are linear combinations of numerical atomic orbitals:[51,52] double zeta for H with polarizations functions (one set of *d*'s) for Si. The basis sets of Ni and Ti include two sets of *s* and *d* orbitals, and one set of *p*'s.

B. Vibrational spectra

The vibrational spectra are obtained from a direct calculation of the force constant matrix (the so-called "frozen-

phonon" approximation) starting with geometries converged down to a maximum force component smaller than 0.003 eV/Å. The dynamical matrices are diagonalized and their orthonormal eigenvectors $e^s_{\alpha i}$ are used to quantify the localization of each normal vibrational mode. Here, α numbers the atom, i the Cartesian coordinate, and s the normal mode. A quantitative measure of the localization is provided by a plot of $L^2_{\{\alpha\}}=(e^s_{\alpha x})^2+(e^s_{\alpha y})^2+(e^s_{\alpha z})^2$ vs ω. The set of atoms $\{\alpha\}$ may be a single atom (e.g., H) or a sum over a group of atoms (e.g., the Si NNs to H).

C. Gap levels

The gap levels are evaluated using our implementation of the marker method.[53,54] The original method predicts the position of donor and acceptor levels in the gap by scaling the calculated ionization energies and electron affinities to those of a "similar" known defect called the marker. In the present case, even isolated interstitial Ti and Ni are electrically very dissimilar even through both reside at a virtually undisturbed T site. Further, it is not clear which known defect is similar to a Ti-H complex for example. In order to remove the dependence of the results on the choice of marker, we use the perfect crystal as the universal marker for all the defects. In other words, the reference donor and acceptor levels are the top of the valence band and the bottom of the conduction band, respectively. This works well for a wide range of defects provided that the defect geometries and the lattice constant of the supercell are carefully optimized in each charge state with a $3\times3\times3$ k-point sampling. This sampling gives converged energies for the supercell size used here.

D. Accuracy of the predictions

Estimating the accuracy of theoretical predictions is an imperfect science. The numbers predicted in this paper involve total energy differences, vibrational frequencies, and gap levels. Comments about the expected accuracy of these predictions are as follows.

Total energy differences are usually reliable because of error compensation. A reasonable error estimate is probably 0.1–0.2 eV at most. For example, the activation energies for diffusion of interstitial transition metals calculated at the same level of theory are all within 0.00 and 0.08 eV from the measured values.[13] Note that none of these migration barriers involves a substantial amount of strain at the transition point (the hexagonal interstitial site). As for the spin states, one compares two essentially identical configurations with different spins. The error in these relative energies should be very small.

The vibrational spectra, calculated at the Γ point, are accurate. It is not unusual to predict local vibrational modes within a few percent of the ones measured at low temperatures (see, for example, Ref. 55). The accuracy of pseudolocal modes is almost impossible to assess because few (if any) of the defects exhibiting phonon sidebands in their photoluminescence spectrum have been identified with certainty. However, the quality of the dynamical matrix is confirmed by the calculations of phonon densities of state, specific heats, and isotope-dependent anomalies in the Debye temperature[56–58] or vibrational lifetimes of localized modes.[59–61]

The predictions of gap levels are more complicated and claiming one typical error bar is misleading. For example, any level too close (within 0.10 eV or so) to a band is unreliable. In our implementation of the marker method (described above), we calculate the position of donor levels relative to the top of the valence band and that of acceptor levels relative to the bottom of the conduction band. This works well in many cases. For example, the average error for the 11 donor and 11 acceptor levels calculated in Refs. 13, 44, 45, and 55 (defects associated with isolated Ti, Fe, and Ni, Fe-acceptor pairs, interstitial C and C-O complexes) is 0.07 eV with a minimum (maximum) error of 0.00 (about 0.15) eV for both types of levels, as compared to the measured values. The error bar on double donor or acceptor levels is expected to be larger.

On the other hand, if a donor level is unusually high in the gap, close to the conduction band (or an acceptor is very low in the gap, close to the valence band) the uncertainty increases because the level may be tagged relative to the wrong band. Examples of such behavior are negative-U centers. None of the defect centers studied here are in this category.

III. Ti-H INTERACTIONS

In p-type Si and in equilibrium, H is positively charged and diffuses as the bond-centered interstitial H^+_{bc}. It is much more likely to trap at negatively charged shallow acceptors than at Ti_i^{++}. Interactions between Ti_i and H are observed only when minority carriers are present[29] and the interacting impurities are in the 0 charge state. This is the situation we are considering here.

A. Structures and binding energies

We find two nearly energetically degenerate Ti-H pairs which we label $\{Ti_iH\}$ and $\{Ti_iH_{bc}\}$, respectively (Fig. 1). $\{Ti_iH\}$ is trigonal with Ti_i at a T site and H bound to it, just beyond the nearest hexagonal interstitial site. The Ti-H overlap population is only 0.12, suggesting a weak Ti-H bond. $\{Ti_iH_{bc}\}$ has no bond between Ti_i and H. One Si atom near Ti moves away from the substitutional site along a trigonal axis, Ti_i moves off the T site and overlaps with it, while H ties up the Si dangling bond. The energy gained by forming a strong Si-H bond and increasing the Ti-Si overlap exceeds the energy cost associated with the large displacement of a Si atom and the breaking of a Si-Si bond.

In the 0 charge state, the binding energies relative to isolated H_{bc} are almost the same for the two defects: $Ti_i+H_{bc}\rightarrow\{Ti_iH\}+0.93$ eV and $Ti_i+H_{bc}\rightarrow\{Ti_iH_{bc}\}+0.91$ eV. These binding energies are consistent with the 570 K annealing temperature reported in the experiments.[29]

Ti_i should not trap a second H interstitial because the formation of an H_2 molecule is energetically favored. In the 0 charge state, $\{Ti_iH\}+H_{bc}\rightarrow\{Ti_iH_2\}+0.86$ eV, but then $\{Ti_iH_2\}\rightarrow Ti_i+H_2+0.28$ eV. A third H interstitial should form $\{Ti_iH\}$ or $\{Ti_iH_{bc}\}+H_2$. However, a fourth H can result in the formation of $\{Ti_iH_4\}$.

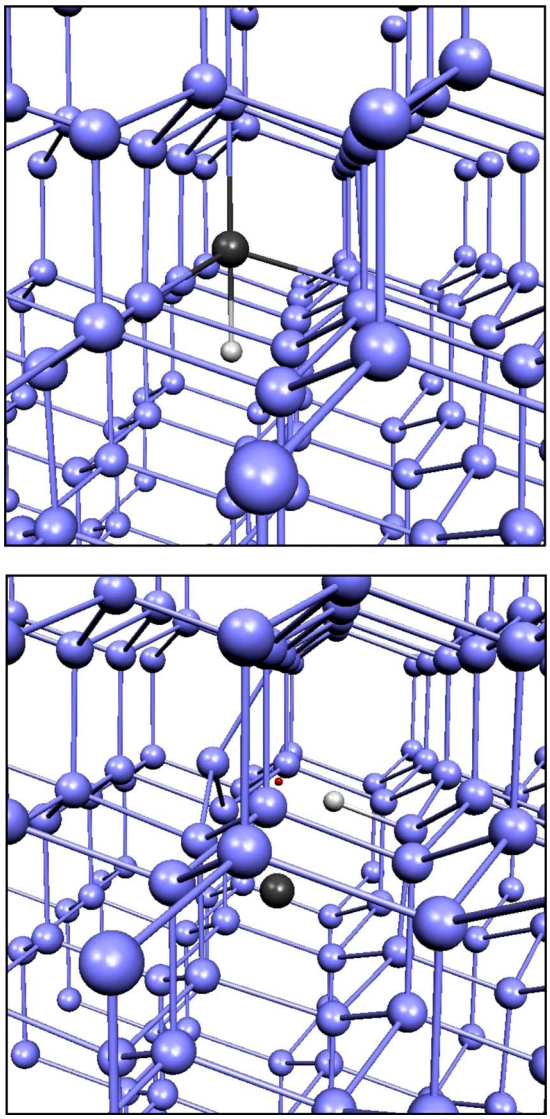

FIG. 1. (Color online) $\{Ti_iH\}$ (top) has H bound to Ti along the trigonal axis. $\{Ti_iH_{bc}\}$ (bottom) has one Si atom displaced from its substitutional site (red dot) while H saturates the other Si dangling bond. Ti is the black sphere, the Si atoms are light blue spheres, and H is the small white sphere.

In the experiments discussed here, hydrogen flows from the surface into the bulk and can therefore accumulate in large concentrations in the subsurface region, which is also where the DLTS measurements are made. Under these conditions, it is therefore possible that H accumulates near Ti_i. The $\{Ti_i,H_4\}$ complex has Ti_i at the T site with four H atoms bound to it along the four trigonal axis pointing away from its four Si NNs. The reaction $Ti_i+2H_2 \rightarrow \{Ti_i,H_4\}$ occurs with the small energy gain of 0.22 eV. $\{Ti_i,H_4\}$ is fully passivated. This is the only electrically inactive Ti-H complex we found in the present study.

B. Calculated and measured gap levels

The calculated gap levels of Ti_i, $\{Ti_iH\}$, and $\{Ti_iH_{bc}\}$ are compared to the measured[29] values in Table I. $\{Ti_iH\}$ has double-donor level at $E_v+0.13$ eV (close to the calculated double-donor level of isolated Ti_i) and a donor level at $E_v+0.78=E_c-0.38$ eV (close to one of the levels assigned to a Ti-H complex). $\{Ti_iH_{bc}\}$ has double-donor and donor levels at $E_v+0.42$ and $E_v+0.54=E_c-0.62$ eV, respectively. The latter is close to the DLTS peak at $E_c-0.57$ eV assigned to a Ti-H complex.

TABLE I. Calculated [measured (Ref. 29)] gap levels (in eV) for Ti_i, $\{Ti_iH\}$, and $\{Ti_iH_{bc}\}$. The top row lists the acceptor levels, the middle row the donor levels, and the bottom row the double donor levels. The two measured levels of Ti-H complexes at $E_c-0.31$ eV and $E_c-0.57$ eV have not been associated with a specific defect. We assign them here to $\{Ti_iH\}$ and $\{Ti_iH_{bc}\}$, respectively.

Ti_i	$\{Ti_iH\}$	$\{Ti_iH_{bc}\}$
$E_c+0.07$ [−0.09]		
$E_v+0.76$ [+0.89]	$E_c-0.38$ [−0.31]	$E_c-0.62$ [−0.57]
$E_v+0.15$ [+0.25]	$E_v+0.13$	$E_v+0.42$

C. Vibrational spectra

Figure 2 shows all the localized vibrational modes of the Ti-H complexes. Upon D substitution, the stretch and wag modes of H in $\{Ti_iH\}$ at 1158 cm^{-1}, 636 cm^{-1}, and 614 cm^{-1} shift to 825 cm^{-1}, 436 cm^{-1}, and 425 cm^{-1}, respectively. In $\{Ti_iH_{bc}\}$, they shift from 1733 cm^{-1},

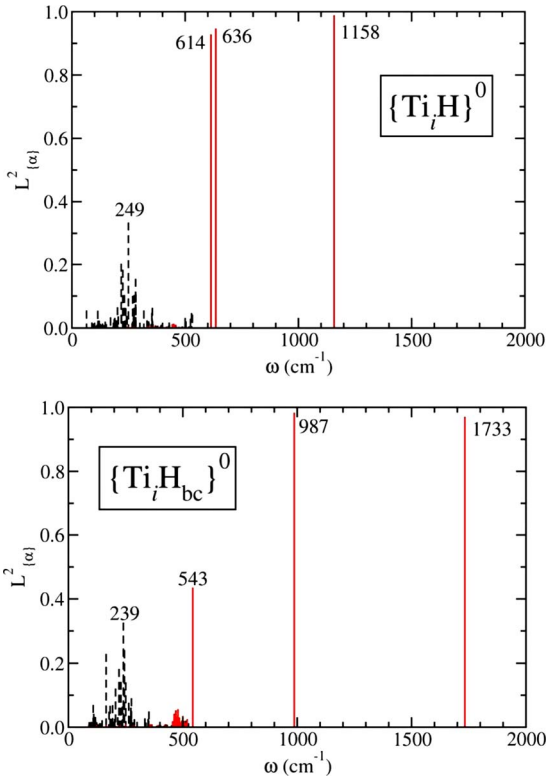

FIG. 2. (Color online) Localization $L^2_{\{\alpha\}}(\omega)$ of the $\{Ti_iH\}$ (top) and $\{Ti_iH_{bc}\}$ (bottom) complexes. The solid (red) lines are for α =H and the (black) dashed line for α=Ti.

987 cm^{-1}, and 543 cm^{-1} to 1246 cm^{-1}, 706 cm^{-1}, and 343 cm^{-1}, respectively.

D. H and substitutional Ti

In the 0 charge state, the interaction of Ti_i with a preexisting vacancy (V) results in the formation of substitutional Ti (Ti_s) with a 2.7 eV energy gain.[13] The formation of Ti_s is not likely to occur in p-type Si under equilibrium conditions since both the vacancy[62] and Ti_i are positively charged. However, these samples were contaminated with Ti during growth and some Ti_s may have formed. The electrical activity of Ti_s has been predicted[13] to be very low with a donor level at $E_v+0.11$ eV. The acceptor level is resonant with the bottom of the conduction band ($E_c-0.03$ eV).

In the 0 charge state, H traps at Ti_s with a gain in energy of 1.54 eV. The resulting $\{Ti_sH\}$ defect has H bound directly to the Ti along a C_{2v} axis. We find a donor ($E_v+0.07$ eV) and two acceptor ($E_c-0.21$ and $E_c-0.10$ eV) levels in the gap. None of them are close to the DLTS levels reported for Ti-H.

The trapping of a second H leads to the formation of $\{Ti_sH_2\}$ with a gain of 1.86 eV. However, instead of binding to Ti, the two H atoms bind to Si atoms in a bonding configuration and the Ti atom moves away from the substitutional site toward the T site. The reaction occurs without activation energy, during a $T=0$ K conjugate gradient geometry optimization. This defect could also be labeled $\{Ti_i, VH_2\}$. This structure has donor and acceptor levels at $E_v+0.05$ and $E_c-0.20$ eV, respectively. These gap levels are not close to the ones reported experimentally for any Ti-H complexes. A third H atom finishes the kick-out process and the result is Ti_i+VH_3, with a gain of 2.12 eV.

IV. Ni-H INTERACTIONS

A. H and interstitial Ni

Our calculations[13,63] show that isolated Ni_i has charge 0 and spin 0 for all positions of the Fermi level. It is not visible by DLTS but could *a priori* trap H and form electrically active pairs or larger complexes. However, the only Ni_i-H "pair" has H at a bond-centered Si-H_{bc}-Si site near Ni_i with no Ni_i-H overlap. In the 0(+) charge state, this configuration is more stable by only 0.38 eV (0.24 eV) than the dissociated species. This energy is smaller than the activation energy for diffusion of H_{bc}, 0.48 eV.[2,3] Since the DLTS peaks associated with Ni-H complexes survive a 470 K anneal, it is most unlikely that this pair plays any role at all in these experiments.

B. H and substitutional Ni

If vacancies are present, Ni_i becomes substitutional (Ni_s) with a 2.7 eV gain in energy. The reaction $Ni_i+V \rightarrow Ni_s$ occurs without an energy barrier.[13] The 2.7 eV energy gain comes from the formation of four Ni-Si covalent bonds, as Ni_s promotes some electrons from the $3d$ to the $4sp$ shell.

1. Structures and binding energies

Interstitial H traps at Ni_s. In the 0 charge state, $Ni_s+H_{bc} \rightarrow \{Ni_sH\}+1.44$ eV, and then $\{Ni_sH\}+H_{bc} \rightarrow \{Ni_sH_2\}+1.39$ eV. The Ni-H bond length is 1.66 Å. $\{Ni_sH_2\}$ is more stable than Ni_s+H_2 by 0.86 eV. The $\{Ni_sH\}$ and $\{Ni_sH_2\}$ complexes are shown in Fig. 3.

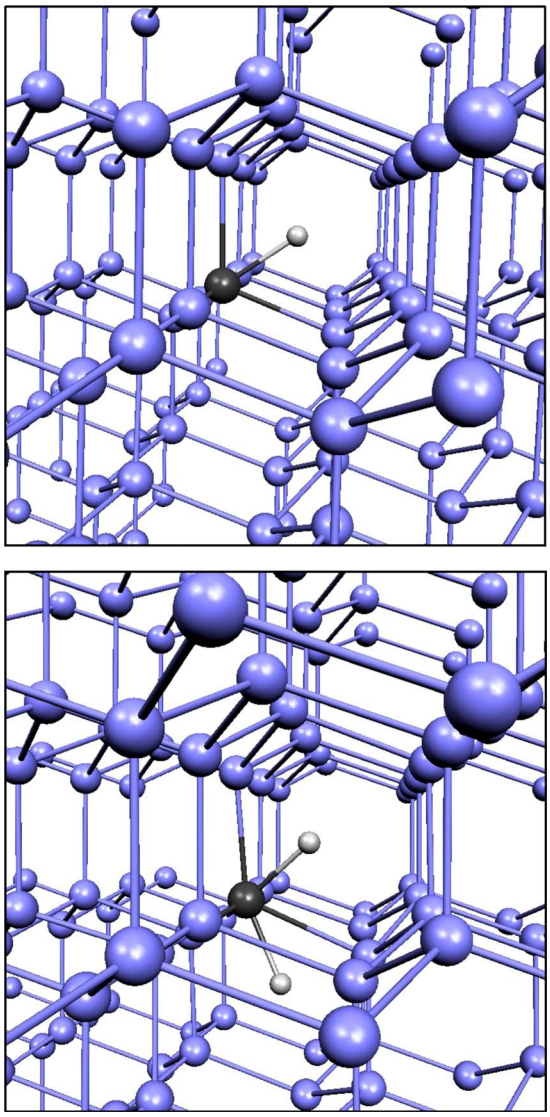

FIG. 3. (Color online) $\{Ni_sH\}$ (top) and $\{Ni_sH_2\}$ (bottom) have the H bound directly to Ni_s, which becomes fivefold and sixfold coordinated, respectively. There is no Si-H overlap. Ni is the black sphere, the Si atoms are light blue spheres, and H is the small white sphere.

If a third H atom interacts with $\{Ni_sH_2\}$, the Ni atom spontaneously moves away from the substitutional site toward the T site with an energy gain of 0.39 eV in the 0 charge state. The reaction occurs without activation energy, during a $T=0$ K conjugate gradient geometry optimization. The result is a partially saturated vacancy VH_3 and the electrically inactive Ni_i. Therefore, there are only two Ni-H complexes involving a single Ni atom.

2. Calculated and measured gap levels

The gap levels of Ni_s have been measured by several groups.[9,32–35] Ni_s has a double acceptor level at $E_c-0.08$ eV, acceptor and donor levels in the range $E_c-0.39$ to

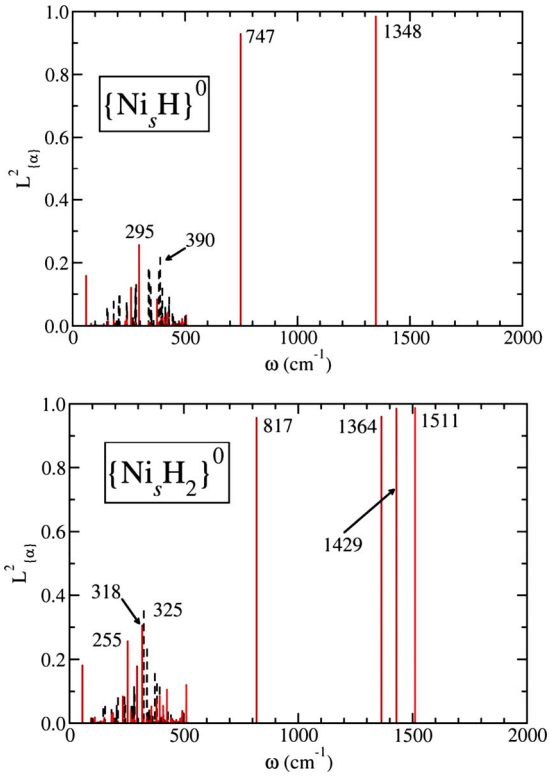

FIG. 4. (Color online) Localization $L^2_{\{\alpha\}}(\omega)$ of the $\{Ni_sH\}$ (top) and $\{Ni_sH_2\}$ (bottom) complexes. The solid red lines are for α=H and the black dashed line for α=Ni.

0.47 and $E_v+0.15$ to 0.18 eV, respectively. We calculate[13,63] these levels to be at $E_c-0.16$, $E_c-0.31$, and $E_v+0.30$ eV, respectively.

Upon hydrogenation, at least eleven new DLTS lines appear: six hole traps at $E_v+0.08$, 0.20, 0.32, 0.37, 0.47, and 0.56 eV, and five electron traps at $E_c-0.15$, 0.16, 0.25, 0.35, and 0.52 eV. Some of these lines could be due to defects containing more than one Ni atom.

$\{Ni_sH\}$ has a four levels in the gap: double acceptor and acceptor levels at $E_c-0.22$ eV and $E_c-0.34$ eV, respectively; double-donor and donor levels at $E_v+0.06$ eV, and $E_v+0.20$ eV, respectively. $\{Ni_sH_2\}$ has only one acceptor level at $E_c-0.24$ eV. Thus, we find a maximum of five new gaps levels associated with complexes of H with one Ni_s atom. We cannot associate our calculated levels with specific observed ones because of the large number of DLTS peaks reported and of the uncertainty associated with the prediction of gap levels.

3. Vibrational spectra

Figure 4 shows the localization of the vibrational modes associated with the $\{Ni_sH\}$ (top) and $\{Ni_sH_2\}$ complexes. Upon D substitution, the H-related modes in $\{Ni_sH\}$ at 1348 cm^{-1}, 747 cm^{-1}, and 295 cm^{-1} shift to 962 cm^{-1}, 555 cm^{-1}, and 226 cm^{-1}, respectively. In $\{Ni_sH_2\}$, they shift from 1511 cm^{-1}, 1429 cm^{-1}, 1364 cm^{-1}, 817 cm^{-1}, 318 cm^{-1}, and 255 cm^{-1} to 1076 cm^{-1}, 1020 cm^{-1}, 984 cm^{-1}, 595 cm^{-1}, 256 cm^{-1}, and 51 cm^{-1}, respectively.

V. KEY POINTS AND DISCUSSION

First-principles theory in the 216 host-atoms supercell has been used to calculate the structural, electrical, and vibrational properties of Ti-H and Ni-H complexes. The electrical properties of the stable structures are compared to published DLTS data and several of the observed defects are identified. Complete vibrational spectra are calculated in order to facilitate future optical identification.

There are four Ti-H complexes, two of which involve Ti_i and the other two Ti_s. The $\{Ti_iH\}$ and $\{Ti_iH_{bc}\}$ complexes are almost energetically degenerate and each of them exhibits double donor and donor levels. The two DLTS peaks at $E_c-0.31$ eV and $E_c-0.57$ eV observed following the hydrogenation of Ti-contaminated samples[29] are close to the donor levels of the $\{Ti_iH\}$ ($E_c-0.38$ eV vs $E_c-0.31$ eV) and $\{Ti_iH_{bc}\}$ ($E_c-0.62$ eV vs $E_c-0.57$ eV) complexes. Their binding energies are 0.93 eV and 0.91 eV, respectively. These values are consistent with the observed annealing behavior (570 K for 3 h). At such temperatures, the free energy contributions to the dissociation are of the order of 0.2 eV.[64] Adding a second hydrogen to Ti_i results in a complex that is unstable against the formation of an interstitial H_2 molecule.

There is no experimental evidence that Ti_s is present in the samples used to get the DLTS data. Should Ti_s be present in the sample, it will trap one or two interstitial H and then become electrically active. None of the calculated gap levels match an observed DLTS peak.

We find no stable Ni_i-H complexes. The most favorable configuration has H_{bc} near Ni_i, with no Ni-H overlap. The binding energies (0.38 eV and 0.24 eV in the 0 and + charge states, respectively) are too small for this defect to be stable at room temperature. However, Ni_s traps one or two H with binding energies of 1.44 eV and 1.39 eV, respectively. $\{Ni_sH\}$ has two acceptor and two donor levels at $E_c-0.22$ eV, $E_c-0.34$ eV, $E_v+0.20$ eV, and $E_v+0.06$ eV, respectively. $\{Ni_sH_2\}$ has only one acceptor level at $E_c-0.24$ eV. Given the uncertainty associated with the prediction of gap levels, we cannot associate any of the calculated levels to one or another of the eleven DLTS lines reported following the hydrogenation of Ni-contaminated samples.[32] However, Ni_i is a very fast-diffusing interstitial which traps a various defects, forms complexes, and silicides. It is possible that defects containing several Ni impurities are present in the samples and that H also interacts with those.

An unexpected result of our calculations is that sufficiently high concentrations of H result in the trapping of multiple H at a substitutional Ti or Ni, which then leads to the H kicking out the TM to the interstitial site, leaving a (partially) H-saturated VH_n defect. The process begins with $n=2$ in the case of Ti and $n=3$ in the case of Ni. Note that a Ti_sH_2 defect would have Ti six-fold coordinated with only four valence electrons. The kick-out process occurs without activation energy. It is likely that this reaction takes place with other substitutional impurities as well and could explain why the VH_4 defect (2222 cm^{-1} infrared line) often appears in samples heavily hydrogenated from a surface layer while $VH_{n<4}$ is only reported in irradiated or implanted samples.

The H-induced kick out of Ni_s explains why the prehydrogenation concentration of Ni_s is reduced in p-type but not

in *n*-type Si after a 570 K anneal. Indeed, $\{Ni_sH_2\}$ must trap a third H in order to become Ni_i which is invisible in DLTS experiments. $\{Ni_sH_2\}$ has an acceptor level but no donor level. Thus, it would be in the 0 charge state in *p*-type Si, could trap the third H, and be expelled from the substitutional site. However, this kick out would not occur in *n*-type Si since $\{Ni_sH_2\}^-$ is unlikely to trap H_T^-. Thus, the initial concentration of DLTS-active Ni_s would be preserved only in *n*-type Si.

In conclusion, the interactions between hydrogen and Ti or Ni impurities in Si result in the formation of a variety of complexes with binding energies on the order of 0.9–1.5 eV. All the Ni-H and Ti-H complexes that involve a single TM impurity are calculated. An identification for the two Ti-H DLTS defects is proposed. Only the $\{Ti_iH_4\}$ complex is passivated. When more than two H interstitials are available, both Ti_s and Ni_s are ejected from the substitutional site and become Ti_i and Ni_i, respectively, leaving a (partially) hydrogenated vacancy.

ACKNOWLEDGMENTS

This work is supported in part by the grant D-1126 from the R. A. Welch Foundation and by a grant from the Silicon Solar Consortium (SiSoC). The High Performance Computer Center at Texas Tech provided generous amounts of computer time.

*stefan.estreicher@ttu.edu

[1] S. J. Pearton, J. W. Corbett, and M. Stavola, *Hydrogen in Crystalline Semiconductors* (Springer, Berlin, 1992).
[2] S. K. Estreicher, Mater. Sci. Eng. R. **14**, 319 (1995).
[3] *Hydrogen in Semiconductors II*, Semiconductors and Semimetals Vol. 61, edited by N. H. Nickel (Academic, San Diego, 1999).
[4] J. I. Hanoka, C. H. Seager, D. J. Sharp, and J. K. G. Panitz, Appl. Phys. Lett. **42**, 618 (1983).
[5] F. Duerinckx and J. Szlufcik, Sol. Energy Mater. Sol. Cells **72**, 231 (2002).
[6] F. Jiang, M. Stavola, A. Rohatgi, D. Kim, J. Holt, H. Atwater, and J. Kalejs, Appl. Phys. Lett. **83**, 931 (2003).
[7] S. Kleekajai, F. Jiang, M. Stavola, V. Yelundur, K. Nakayashiki, A. Rohatgi, G. Hahn, S. Seren, and J. Kalejs, J. Appl. Phys. **100**, 093517 (2006).
[8] E. R. Weber, Appl. Phys. A **30**, 1 (1983).
[9] A. A. Istratov and E. R. Weber, Appl. Phys. A: Mater. Sci. Process. **66**, 123 (1998).
[10] A. A. Istratov, H. Hieslmair, and E. R. Weber, Appl. Phys. A: Mater. Sci. Process. **69**, 13 (1999).
[11] A. A. Istratov, H. Hieslmair, and E. R. Weber, Appl. Phys. A: Mater. Sci. Process. **70**, 489 (2000).
[12] A. A. Istratov, C. Flink, H. Hieslmair, E. R. Weber, and T. Heiser, Phys. Rev. Lett. **81**, 1243 (1998).
[13] D. J. Backlund and S. K. Estreicher, Phys. Rev. B **81**, 235213 (2010).
[14] A. A. Istratov, C. Flink, H. Hieslmair, T. Heiser, and E. R. Weber, Appl. Phys. Lett. **71**, 2121 (1997).
[15] M. Seibt, H. Hedemann, A. A. Istratov, F. Riedel, A. Sattler, and W. Schröter, Phys. Status Solidi A **171**, 301 (1999).
[16] T. Buonassisi, A. A. Istratov, M. D. Pickett, M. A. Marcus, T. F. Ciszek, and E. R. Weber, Appl. Phys. Lett. **89**, 042102 (2006).
[17] W. Wang, D. Yang, X. Ma, and D. Que, J. Appl. Phys. **103**, 093534 (2008).
[18] H. Savin, M. Yli-Koski, and A. Haarahhiltunen, Appl. Phys. Lett. **95**, 152111 (2009).
[19] J. Weber, in *Hydrogen in Semiconductors and Metals*, edited by N. H. Nickel, W. B. Jackson, R. C. Bowman, and R. Leisure, MRS Symposia Proceedings No. 513 (Materials Research Society, Warrendale, PA, 1998), p. 345.
[20] J.-U. Sachse, E. Ö. Sveinbjörnsson, N. Yarykin, and J. Weber, Mater. Sci. Eng., B **58**, 134 (1999).
[21] J.-U. Sachse, E. Ö. Sveinbjörnsson, W. Jost, J. Weber, and H. Lemke, Phys. Rev. B **55**, 16176 (1997).
[22] J.-U. Sachse, J. Weber, and E. Ö. Sveinbjörnsson, Phys. Rev. B **60**, 1474 (1999).
[23] A. C. Wang and C. T. Sah, J. Appl. Phys. **56**, 1021 (1984).
[24] K. Graff, *Metal Impurities in Silicon-Device Fabrication* (Springer, Berlin, 1995).
[25] S. Hocine and D. Mathiot, Appl. Phys. Lett. **53**, 1269 (1988).
[26] A. Rohatgi, J. R. Davis, R. H. Hopkins, P. Rai-Choudhury, P. G. McMullin, and J. M. R. McCormick, Solid-State Electron. **23**, 415 (1980).
[27] J. T. Borenstein, J. I. Hanoka, B. R. Bathey, J. P. Kalejs, and S. Mil'shtein, Appl. Phys. Lett. **62**, 1615 (1993).
[28] R. Singh, S. J. Fronash, and A. Rohatgi, Appl. Phys. Lett. **49**, 800 (1986).
[29] W. Jost and J. Weber, Phys. Rev. B **54**, R11038 (1996).
[30] D. E. Woon, D. S. Marynick, and S. K. Estreicher, Phys. Rev. B **45**, 13383 (1992).
[31] F. H. M. Spit, D. Gupta, and K. N. Tu, Phys. Rev. B **39**, 1255 (1989).
[32] M. Shiraishi, J.-U. Sachse, H. Lemke, and J. Weber, Mater. Sci. Eng., B **58**, 130 (1999).
[33] S. J. Pearton and A. J. Tavendale, J. Appl. Phys. **54**, 1375 (1983).
[34] H. Kitagawa and H. Nakashima, Phys. Status Solidi A **99**, K49 (1987); Jpn. J. Appl. Phys., Part 1 **28**, 305 (1989).
[35] H. Lemke, Mater. Sci. Forum **196-201**, 683 (1995).
[36] R. Jones, S. Öberg, J. Goss, P. R. Briddon, and A. Resende, Phys. Rev. Lett. **75**, 2734 (1995).
[37] R. Jones (private communication).
[38] S. K. Estreicher, D. West, and P. Ordejón, Solid State Phenom. **82-84**, 341 (2002).
[39] D. West, S. K. Estreicher, S. Knack, and J. Weber, Phys. Rev. B **68**, 035210 (2003).
[40] D. J. Backlund and S. K. Estreicher, in *Defects in Inorganic Photovoltaic Materials*, edited by D. Friedman, M. Stavola, W. Walukiewicz, and S. Zhang, MRS Symposia Proceedings No. 1268 (Materials Research Society, Warrendale, PA, 2010), p. EE-05.
[41] *Theory of Defects in Semiconductors*, edited by D. A. Drabold

and S. K. Estreicher (Springer, Berlin, 2007).
[42] D. Sánchez-Portal, P. Ordejón, E. Artacho, and J. M. Soler, Int. J. Quantum Chem. **65**, 453 (1997).
[43] E. Artacho, D. Sánchez-Portal, P. Ordejón, A. García, and J. M. Soler, Phys. Status Solidi B **215**, 809 (1999).
[44] S. K. Estreicher, M. Sanati, and N. Gonzalez Szwacki, Phys. Rev. B **77**, 125214 (2008).
[45] M. Sanati, N. Gonzalez Szwacki, and S. K. Estreicher, Phys. Rev. B **76**, 125204 (2007).
[46] H. J. Monkhorst and J. D. Pack, Phys. Rev. B **13**, 5188 (1976).
[47] N. Troullier and J. L. Martins, Phys. Rev. B **43**, 1993 (1991).
[48] L. Kleinman and D. M. Bylander, Phys. Rev. Lett. **48**, 1425 (1982).
[49] V. L. Moruzzi and C. B. Sommers, *Calculated Electronic Properties of Ordered Alloys: A Handbook* (World Scientific, Singapore, 1995).
[50] J. P. Perdew, K. Burke, and M. Ernzerhof, Phys. Rev. Lett. **77**, 3865 (1996).
[51] O. F. Sankey and D. J. Niklewski, Phys. Rev. B **40**, 3979 (1989).
[52] O. F. Sankey, D. J. Niklewski, D. A. Drabold, and J. D. Dow, Phys. Rev. B **41**, 12750 (1990).
[53] A. Resende, R. Jones, S. Öberg, and P. R. Briddon, Phys. Rev. Lett. **82**, 2111 (1999).
[54] J. P. Goss, M. J. Shaw, and P. R. Briddon in Ref. 41, p. 69.
[55] D. J. Backlund and S. K. Estreicher, Phys. Rev. B **77**, 205205 (2008).
[56] M. Cardona, R. K. Kremer, M. Sanati, S. K. Estreicher, and T. R. Anthony, Solid State Commun. **133**, 465 (2005).
[57] M. Sanati and S. K. Estreicher, J. Phys.: Condens. Matter **16**, L327 (2004).
[58] R. K. Kremer, M. Cardona, E. Schmitt, J. Blumm, S. K. Estreicher, M. Sanati, M. Bockowski, I. Grzegory, T. Suski, and A. Jezowski, Phys. Rev. B **72**, 075209 (2005).
[59] D. West and S. K. Estreicher, Phys. Rev. Lett. **96**, 115504 (2006).
[60] K. K. Kohli, G. Davies, N. Q. Vinh, D. West, S. K. Estreicher, T. Gregorkiewicz, I. Izeddin, and K. M. Itoh, Phys. Rev. Lett. **96**, 225503 (2006).
[61] D. West and S. K. Estreicher, Phys. Rev. B **75**, 075206 (2007).
[62] G. D. Watkins, in *Handbook of Semiconductor Technology, Electronic Structure and Properties of Semiconductors*, edited by K. A. Jackson and W. Schroeter (Wiley-VCH, Weinheim, 2000), Vol. 1, Chap. 3.
[63] S. K. Estreicher and D. J. Backlund, in *Defects in Inorganic Photovoltaic Materials*, edited by D. Friedman, M. Stavola, W. Walukiewicz, and S. Zhang, MRS Symposia Proceedings No. 1268 (Materials Research Society, Warrendale, PA, 2010), p. EE-02.
[64] S. K. Estreicher, M. Sanati, D. West, and F. Ruymgaart, Phys. Rev. B **70**, 125209 (2004).